

Size and concentration effects in the optical properties of alloyed $(\text{Au}_x\text{Ag}_{1-x})_n$ and core-shell $(\text{Ni}_x\text{Ag}_{1-x})_n$ embedded clusters

M. Gaudry^{1,a}, J. Lermé¹, E. Cottancin¹, M. Pellarin¹, B. Prével², M. Treilleux², P. Mélinon², J.-L. Rousset³, and M. Broyer¹

¹ Laboratoire de Spectrométrie Ionique et Moléculaire, CNRS and Université Lyon I, bâtiment Kastler, 43 boulevard du 11 novembre 1918, 69622 Villeurbanne Cedex, France

² Département de Physique des Matériaux, CNRS and Université Lyon I, bâtiment Brillouin, 43 boulevard du 11 novembre 1918, 69622 Villeurbanne Cedex, France

³ Institut de Recherche sur la Catalyse, CNRS, 2 avenue Albert Einstein, 69626 Villeurbanne Cedex, France

Received 21 November 2000

Abstract. Optical properties of mixed clusters $(\text{Au}_x\text{Ag}_{1-x})_n$ and $(\text{Ni}_x\text{Ag}_{1-x})_n$, produced by laser vaporization and embedded in an alumina matrix, are reported. The size effects are investigated for different concentrations ($x = 0.25, 0.5$ and 0.75) in the diameter range 2–4 nm. For alloyed clusters $(\text{Au}_x\text{Ag}_{1-x})_n$ of a given size an almost linear evolution of the surface plasmon frequency ω_s with the concentration is observed (between those of pure gold and pure silver clusters). Moreover the blue-shift and the damping of the resonance with decreasing size is all the more important as the gold concentration in the particles increases. Such results are in agreement with theoretical calculations carried out in the frame of the time-dependent local-density-approximation (TDLDA) including an inner skin of ineffective screening and the porosity of the matrix. The optical response of $(\text{Ni}_x\text{Ag}_{1-x})_n$ clusters exhibits a surface plasmon resonance in the same spectral range as the one observed for pure silver clusters, but considerably damped and broadened. For a given mean cluster size 3.0 nm, a blue-shift of the resonance is observed when increasing the nickel concentration (between $x = 0.25$ and $x = 0.75$). The results are in good qualitative agreement with classical predictions in the dipolar approximation, assuming a core-shell geometry.

PACS. 36.40.Vz Optical properties of clusters – 36.40.-c Atomic and molecular clusters – 36.40.Gk Plasma and collective effects in clusters – 73.50.Mx High-frequency effects; plasma effects

1 Introduction

Optical absorption has proven to be a sensitive tool in the study of small metal particles [1]. In the nanosized domain the optical response of a metal cluster is dominated by the surface plasmon resonance. Its position and width depend on the particle size due to finite-size quantum effects. In the case of noble metals like gold and silver, the response of the valence electrons is influenced by the polarization of the d-core electrons through screening effects. The interpretation of optical properties of noble metal clusters is now well understood and results on embedded gold and silver clusters are well reproduced by time-dependent-local-density-approximation (TDLDA) calculations taking into account the polarization of the d electrons in a two region dielectric model [2,3] and the porosity of the matrix [4–6].

This study intends to probe mixed embedded $(\text{Au}_x\text{Ag}_{1-x})_n$ and $(\text{Ni}_x\text{Ag}_{1-x})_n$ particles below 4 nm in diameter for various relative concentrations x . The clusters $(\text{Au}_x\text{Ag}_{1-x})_n$ have been already studied for $x = 0.5$ and

their optical properties (surface plasmon resonance, blue-shift and damping with decreasing cluster size) were found intermediate between those of pure gold and pure silver clusters [7]. For a more complete review of the works on the Au/Ag nano-system we refer the reader to this publication and the references cited therein. Calculations based on the TDLDA formalism were found to be in good agreement with the experimental results although the model used for evaluating the dielectric function of the ionic background was rather crude.

The first part of this paper reports the composition and size effects in the optical properties of $(\text{Au}_x\text{Ag}_{1-x})_n$ clusters ($x = 0.25, 0.5, 0.75$). The second part concerns the bimetallic $(\text{Ni}_x\text{Ag}_{1-x})_n$ clusters that form a core-shell geometry [8]. The evolution of the plasmon resonance is studied with respect to composition and size.

The paper is planned as follows. After a recall of the sample production and characterizations in section 2, section 3 shows the results obtained for $(\text{Au}_x\text{Ag}_{1-x})_n$ and $(\text{Ni}_x\text{Ag}_{1-x})_n$ clusters. The results for the first system are compared to TDLDA based calculations and for the

^a e-mail: mgaudry@lasim.univ-lyon1.fr

second one to simple classical calculations within the quasi-static approximation.

2 Experiments

The sample preparation and their characterizations are not discussed in detail as they have been described elsewhere [4–7]. Therefore we only outline the main steps of fabrication of the nanostructured films.

Clusters are produced with a laser vaporization source using a continuous flow of inert gas (helium). By varying this pressure between 20 and 60 mbar one can change the mean cluster size. Briefly, a frequency doubled Nd:YAG pulsed laser ($\lambda = 532$ nm) is focused onto a rod of an alloy $\text{Au}_x\text{Ag}_{1-x}$ or $\text{Ni}_x\text{Ag}_{1-x}$ in a small chamber (x is the atomic concentration of gold or nickel). The produced metallic plasma, cooled by helium gas, combines into clusters and expands through a nozzle. The so-formed clusters are then collimated through a skimmer into a high vacuum chamber (10^{-7} mbar) and co-deposited with the transparent alumina matrix (evaporated by an electron gun) on various substrates depending on the measurements to be performed. The metal concentration of the sample lies below 5% and the alumina matrix was found to be porous, amorphous and transparent up to 5 eV. Rutherford Back Scattering (RBS) and energy-dispersive X-ray (EDX) measurements give the same averaged composition in our samples as in the alloy targets. The size distributions of the clusters, determined by Transmission Electron Microscopy (TEM), follow a log-normal law and the micrographs reveal almost spherical particles whose sizes vary from 1.7 to 4 nm in diameter.

Absorption measurements are performed on the films deposited on pure silica (suprasil) substrates with a Perkin-Elmer spectrophotometer, in a spectral range 248–800 nm (1.55–5.0 eV).

Besides, Low-Energy Ion Scattering (LEIS) experiments have been performed on the clusters $(\text{Ni}_{0.5}\text{Ag}_{0.5})_n$ (under ultra-high vacuum) in order to study the surface composition of these mixed particles of immiscible metals [8]. The preliminary analyses show that silver atoms cover the surface of the clusters confirming thus the segregation effect.

3 Results and discussion

3.1 The system $\text{Au}_x\text{Ag}_{1-x}$

Figure 1 shows the experimental absorption spectra for two different compositions $x = 0.25$ and $x = 0.75$.

In all spectra one can see a resonance peak between 2 and 3 eV corresponding to the surface plasmon resonance and a raising of the absorption for higher energies attributed to interband transitions. For larger clusters the position of the surface plasmon frequency $\omega_s((\text{Au}_x\text{Ag}_{1-x})_n)$ corresponds almost to the formula:

$$\omega_s((\text{Au}_x\text{Ag}_{1-x})_n) = x\omega_s(\text{Au}_n) + (1-x)\omega_s(\text{Ag}_n).$$

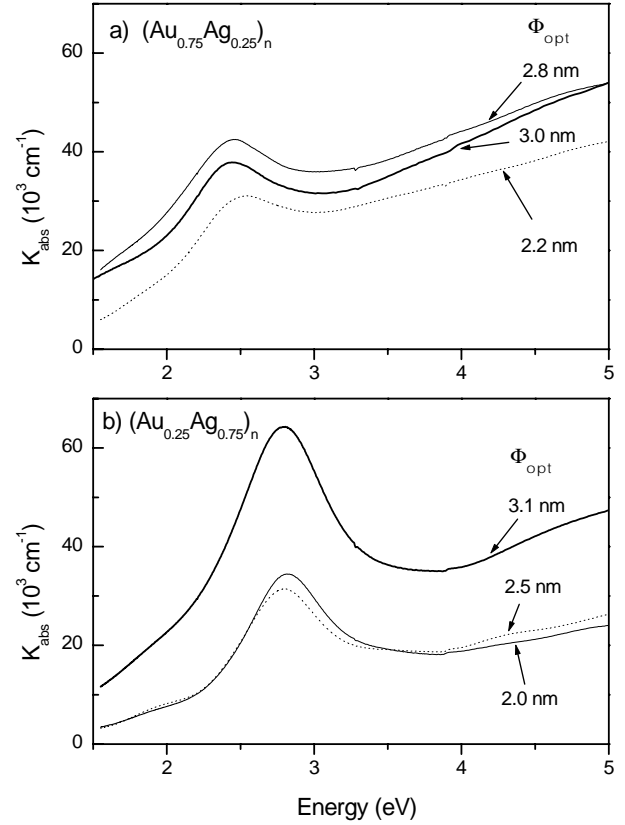


Fig. 1. Absorption spectra of gold-silver embedded clusters. $\langle\phi\rangle$ designs the mean cluster diameter and $\phi_{opt} = \langle\phi^3\rangle^{1/3}$:

| | | thick line | thin line | dotted line |
|------------|---------------------------------|------------|-----------|-------------|
| $x = 0.75$ | $\langle\phi\rangle/\phi_{opt}$ | 2.8/3.0 | 2.7/2.8 | 2.1/2.2 |
| $x = 0.25$ | $\langle\phi\rangle/\phi_{opt}$ | 2.9/3.1 | 2.3/2.5 | 1.9/2.0 |

This almost linear evolution of ω_s with the concentration is in agreement with the results obtained by Papavassilou, Link *et al.* but disagrees with those of Teo *et al.* [9–11]. However, in contrast to these studies, the cluster diameter in our samples is always smaller than 5 nm. The resonance band is more pronounced for the clusters containing only 25% gold whereas it appears strongly damped when they have 75% gold which indicates a more important coupling between intra- and interband transitions with increasing x . For $x = 0.25$ no size effects are obvious whereas a noticeable blue-shift with decreasing cluster size appears for $x = 0.75$. The importance of this blue-shift is halfway between the ones observed in pure gold and mixed $(\text{Au}_{0.5}\text{Ag}_{0.5})_n$ embedded clusters [7].

In Figure 2 is displayed the size evolution of the maximum of the plasmon peak obtained experimentally and theoretically. Experimentally one can see that the size effects progress steadily with the gold concentration. The blue-shift with decreasing size weakens with increasing concentration of silver atoms inside the clusters and is completely quenched for $x = 0.25$ (75% silver). These results are in good agreement with calculations based on the

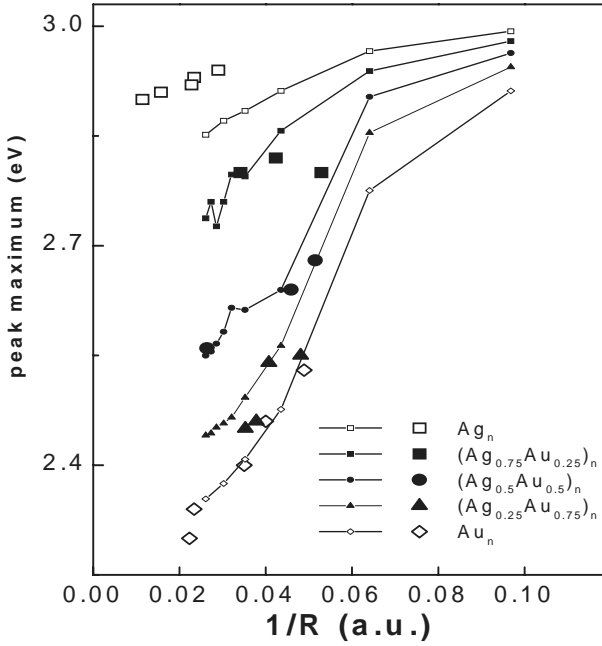


Fig. 2. Size evolution of the peak plasmon maximum for different concentrations in embedded $(\text{Au}_x \text{Ag}_{1-x})_n$ clusters ($R = \frac{\phi_{opt}}{2}$). Lines with small and large symbols correspond respectively to TDLDA and experimental results.

TDLDA formalism. In this model the s-valence electrons are quantum mechanically treated whereas the ionic metal background is phenomenologically described by both a *jellium* (positive charge distribution) of radius $R = r_s N^{\frac{1}{3}}$ (where r_s is the Wigner-Seitz radius) and a homogeneous dielectric medium extending up to $R_1 = R - d$ (d is the thickness of the inner skin of ineffective screening). The alumina matrix is also described macroscopically through its dielectric function ϵ_m [12]. Moreover the local porosity at the cluster-matrix interface is taken into account *via* a vacuum rind of thickness d_m . The parameter values taken in the present calculations are the same as the ones used for pure silver and gold embedded clusters, namely $d(\text{Au}_x \text{Ag}_{1-x}) = d(\text{Ag}) = d(\text{Au}) = 3.5$ a.u. and $d_m = 2$ a.u. [6]. The main difficulty is to estimate the dielectric function of the mixed particles $(\text{Au}_x \text{Ag}_{1-x})_n$. In the present work the dielectric function of the ionic background in the composite particles $(\text{Au}_x \text{Ag}_{1-x})_n$ consists in taking the composition weighted average of the d-electrons dielectric functions of the constituent metals:

$$\epsilon_{(\text{Au}_x \text{Ag}_{1-x})_n}^d(\omega) = x\epsilon_{\text{Au}}^d(\omega) + (1-x)\epsilon_{\text{Ag}}^d(\omega).$$

This problem has been extensively discussed in the study devoted to embedded $(\text{Au}_{0.5} \text{Ag}_{0.5})_n$ clusters [7]. Firstly, the facility of these two materials for alloying at any concentration leads to think that the clusters leaving the source are globally homogeneous. Secondly, provided that the mixed clusters can be pictured as a stacking of small Au and Ag domains (no segregation) that can be described by dielectric constants equal or close to those of both pure materials Au and Ag, this assumption is suitable for

$x = 0.5$ [13]. Nevertheless this assumption is more open to criticism for concentrations far from $x = 0.5$.

The model gives the position of the plasmon resonance in reasonable agreement with the experimental results and the size effects are well reproduced, except for $x = 0.25$ for which no size effects are observed experimentally although the model overestimates a noticeable one. It seems that the model overestimates the size effects for high silver concentrations. However, we can underline that the mean experimental slopes are similar to the theoretical ones for $x = 0.5, 0.75$ and 1.0 (see figure 2).

The work as a whole on $(\text{Au}_x \text{Ag}_{1-x})_n$ embedded clusters will be developed in a forthcoming paper [15] where other assumptions for the dielectric function of the composite particles will be proposed.

3.2 The system $\text{Ni}_x \text{Ag}_{1-x}$

To our knowledge, the system Ag/Ni has never been studied in the nanosized domain but silver and nickel are known to be immiscible metals. The LEIS measurements bring the same conclusion for our clusters, *i.e.* the silver atoms move onto the surface of the mixed particles. This phenomenon can be explained by the lower surface energy of silver compared to nickel.

The absorption measurements have been performed for different compositions ($x = 0.25, 0.5, 0.75$). In all the spectra where a surface plasmon resonance occurs one can see that this resonance is almost in the same spectral range as the one obtained for pure silver clusters but it is considerably broadened. A Mie-like calculation with two interfaces is in accordance with our results. Moreover, by calculating the respective absorption of silver and nickel one obtains that the plasmon band is exhausted by light absorption in both metals, even if pure nickel clusters do not exhibit any surface plasmon resonance band [14]. By adding a small amount of silver, the effective dielectric function is modified and resonance conditions over the entire volume occur, in the very spectral range of the plasmon excitation of the silver metal particle.

In Figure 3a are displayed, for almost the same mean size ($3.0 < \phi_{moy} < 3.3$ nm), absorption spectra of embedded $(\text{Ni}_x \text{Ag}_{1-x})_n$ clusters for three different compositions ($x = 0.25, 0.5, 0.75$) and of pure silver clusters ($x = 0$). The absorption spectra of pure nickel clusters have been recorded and no resonance has been observed. When the concentration of silver increases a large resonance appears, clearly when the concentration of silver exceeds 50% ($x \leq 0.5$). For $x = 0.75$, the amount of silver does not seem to be large enough so that a resonance peak could emerge. Furthermore a blue-shift of the resonance is observed when increasing the nickel concentration from $x = 0.25$ to $x = 0.5$.

These experimental spectra are compared to those obtained within the extended Mie theory in the dipolar approximation, either for a homogeneous sphere (case of pure silver) or for a core-shell Ni-Ag particle, embedded in alumina. In the model the experimental dielectric functions of

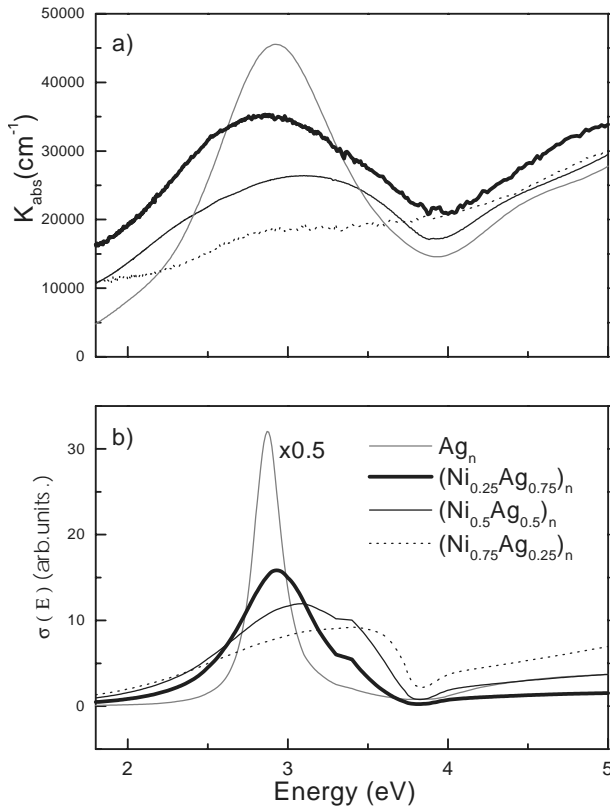


Fig. 3. Absorption spectra of silver-coated nickel clusters. (a) Evolution of absorption spectra (for clusters of almost same mean diameter 3 nm) with the concentration of nickel: Ag_n (gray line; $\langle\phi\rangle = 3.2$ nm); $(\text{Ni}_{0.25}\text{Ag}_{0.75})_n$ (thick line; $\langle\phi\rangle = 3.1$ nm); $(\text{Ni}_{0.5}\text{Ag}_{0.5})_n$ (thin line; $\langle\phi\rangle = 3.3$ nm); $(\text{Ni}_{0.75}\text{Ag}_{0.25})_n$ (dotted line; $\langle\phi\rangle = 3.0$ nm). (b) Absorption cross sections calculated within the Mie-like theory involving two interfaces for different concentrations: Ag_n (gray line); $(\text{Ni}_{0.25}\text{Ag}_{0.75})_n$ (thick line; $f_v = 0.177$); $(\text{Ni}_{0.5}\text{Ag}_{0.5})_n$ (thin line; $f_v = 0.392$); $(\text{Ni}_{0.75}\text{Ag}_{0.25})_n$ (dotted line; $f_v = 0.659$).

the metals [11] and of porous alumina (measured by ellipsometry [4]) have been used. For a core-shell particle the absorption spectrum depends only on the volumic ratio $f_v = \left(\frac{R_c}{R}\right)^3$, except for a scaling factor proportional to R^3 (R_c is the core radius and R is the total radius of the particle). Using the atomic Wigner-Seitz radius of nickel and silver in the bulk ($r_s \approx 2.6$ a.u. and $r_s \approx 3.02$ a.u., respectively), the volumic ratio f_v can be deduced from the atomic composition x . Calculations have been performed using the same radius R , regardless of the composition.

In figure 3b are displayed the calculated absorption spectra for different concentrations ($x = 0.0; 0.25; 0.5; 0.75$). Obviously the theoretical spectra do not reproduce the experimental broadening owing to the size, shape and local-porosity distributions in our samples, but also because we used the dielectric functions of the bulk which underestimate the damping constant Γ characterizing the conduction electron collisions in the particle [1]. When the

particles contain a small amount of nickel ($x = 0.25$), the surface plasmon resonance remains in the same spectral range compared to the one obtained for pure silver but is considerably widened and damped. When the nickel composition increases, the resonance is much more damped.

The size effects have been also studied for $(\text{Ni}_{0.5}\text{Ag}_{0.5})_n$ clusters of diameter between 1.7 and 3.8 nm. The first results show that the absorption resonance weakens with decreasing cluster size. Such results are not predicted by a classical core-shell model for which no size effects are expected, except if the limited electron mean free path effect is taken into account. Besides this effect, this weakening might be due to a change in the structure of the clusters: small clusters are maybe not segregated. Indeed, the amount of silver is not sufficient to form a complete shell around the nickel core.

4 Conclusion

To summarize, the optical properties of mixed embedded $(\text{Au}_x\text{Ag}_{1-x})_n$ particles are intermediate between those of pure gold and pure silver ones. The position of the plasmon resonance moves linearly with the concentration of gold and the blue-shift with decreasing cluster size is all the more important as the gold concentration increases. The calculations based on a TDLDA formalism are in quite good agreement with the experimental results.

Concerning the $(\text{Ni}_x\text{Ag}_{1-x})_n$ clusters, absorption spectra show a resonance peak at the same position as the one observed for pure silver clusters but damped and broadened. These concentration effects have to be extended for other mean sizes. Furthermore it would be also interesting to study the evolution of the absorption with the size for different concentrations. Current works are towards this direction.

References

1. U. Kreibig, M. Vollmer, *Optical properties of metal clusters* (Springer, Berlin, 1995).
2. A. Liebsch, Phys. Rev. B **48**, 11317 (1993).
3. V.V. Krésin, Phys. Rev. B **51**, 1844 (1995).
4. B. Palpant *et al.*, Phys. Rev. B **57**, 1963 (1998).
5. J. Lermé *et al.*, Eur. Phys. J. D **4**, 95 (1998).
6. J. Lermé *et al.*, Phys. Rev. Lett. **80**, 5105 (1998).
7. E. Cottancin *et al.*, Phys. Rev. B **62**, 5179 (2000).
8. J.L. Rousset *et al.*, J. Phys. Chem. B **62**, 5430 (2000).
9. G.C. Papavassiliou, J. Phys. F **6**, L103 (1976).
10. S. Link *et al.*, J. Phys. Chem **103**, 3529 (1999).
11. B.K. Teo *et al.*, J. Am. Chem. Soc. **109**, 3494 (1987).
12. E.D. Palik, *Handbook of optical constants of solids* (Academic Press, Orlando, 1985/1991).
13. W.F.J. Brown, J. Chem. Phys. **23**, 1514 (1995).
14. J. Lermé *et al.*, submitted to J. Chem. Phys.
15. M. Gaudry *et al.*, Phys. Rev. B (to be published).